



## SELECTIVE SEISMIC REHABILITATION OF RC INTERIOR BEAM-COLUMN JOINTS WITH FRP COMPOSITES

Y. Okahashi <sup>1</sup>, C. P. Pantelides <sup>2</sup>, and L.D. Reaveley <sup>3</sup>

### ABSTRACT

The paper is focused on the seismic rehabilitation of RC interior beam column joints with FRP composites. The interior beam-column joints were selected based on deficient details, typical of RC frame buildings built before the 1970's. Two types of beam-column joints were tested: Type I had a 406x610 mm beam and Type II had a 406x406 mm beam. Both joint types had a column with dimensions of 406x406 mm. The reinforcement details for both joint types were such that the beam bottom steel bars at the joint had an embedment of only 127 mm on each side from the face of the column, which created unfavorable conditions for bond development of these bars. In addition, there was no horizontal hoop steel in the joint itself, which created unfavorable conditions for developing the shear strength of the joint. The column vertical steel ratio was 2% with lap splices located immediately above the floor level in the zone of maximum seismic moment, along with widely spaced column ties. The seismic rehabilitation measures with FRP composites were successful in promoting ductile behavior by delaying brittle joint shear failure for Type I joints; however, pullout of the beam bottom steel bars at the joint was still a dominant failure mode for the Type II joints. An equilibrium-based strut-and-tie model was developed for the as-built and FRP rehabilitated joints.

### Introduction

Strengthening of RC beam-column interior joints in building frames which are deficient under seismic loads either in joint shear, or pullout failure of the beam bottom steel bars at the joint, is addressed using carbon Fiber Reinforced Polymer (FRP) composite jackets. FRP composite materials offer significant advantages such as fast installation, high strength/weight ratio, and resistance to corrosion. Rehabilitation of RC beam-column joints using FRP jackets for improving joint shear strength in RC joints, has been studied by Pantelides et al. (1999), Gergely et al. (2000), Mosallam (2000), Ghobarah and Said (2002), Clyde and Pantelides (2002), Antonopoulos and Triantafillou (2003), Prota et al. (2004), Ghobarah and El-Amoury (2005), Pampanin et al. (2007), and Al-Salloum and Almusallam (2007).

<sup>1</sup> CoreBrace, Inc., West Jordan, UT 84088

<sup>2,3</sup> Prof., Dept. of Civil and Envr. Eng., Univ. of Utah, Salt Lake City, UT 84112

The design of the seismic rehabilitation of two types of RC interior beam-column joints with FRP composites is presented in this research. A comparison of the flexural capacity of the beams framing into the joint, and the joint shear strength coefficient of the as-built and rehabilitated joints is provided. In addition, a strut-and-tie model of the beam-column joint discontinuity region is presented for the as-built and FRP rehabilitated joints. The interior beam-column joints under consideration had reinforcement details that were deficient by current seismic standards in two respects: (a) no transverse steel reinforcement was provided in the joint, and (b) the bottom beam steel reinforcement was discontinuous and was terminated 127 mm into the column on both sides. Two types of interior beam-column joints were tested for a total of eight beam-column joint specimens: the first type had a beam depth of 406 mm; the second type had a beam depth of 610 mm; the column was 406 mm square for both joint types. An equilibrium-based strut-and-tie model was developed in this research which was supplemented with strain readings from the internal steel reinforcement and external FRP composite laminates. The strut-and-tie model is shown to predict the joint shear capacity of both joint types with good accuracy and could be used in the seismic rehabilitation of deficient beam-column joints with FRP composites.

### **Strengthening Interior Beam-Column Joints with FRP Composites**

Two types of beam-column joints were tested in this research. Type I had a beam 406 mm wide and 610 mm deep as shown in **Fig. 1(a)**, and Type II had a beam 406 mm wide and 406 mm deep as shown in **Fig. 1(b)**. Both joint types had a column with dimensions of 406x406 mm. The reinforcement details are shown in **Fig. 1**; for both joint types, the beam bottom steel bars at the joint have an embedment of only 127 mm on each side from the face of the column, which creates difficulties for bond development of these bars. In addition, there is no horizontal hoop steel in the joint itself, which creates difficulties for developing the shear strength of the joint. The column vertical steel ratio was 2% with lap splices located immediately above the floor level in the zone of maximum seismic moment, along with widely spaced column ties. Two Type I joints were tested in the as-built condition and two joints were rehabilitated with carbon FRP composites; one Type II joint was tested in the as-built condition and three joints were rehabilitated with carbon FRP composites.

The goals of the FRP composite seismic rehabilitation were to improve the story shear capacity, displacement ductility, energy dissipation, and inelastic rotation capacity of the joints under simulated seismic loads. The main FRP composite elements were designed as follows. To improve the bond of beam bottom steel bars at the joint, and to limit bar slippage, an external FRP “lap splice” technique was implemented. This consisted of applying two 254 mm-wide FRP sheets on each of the unconfined faces in the lower portion of the joint. The first FRP sheet applied was 914 mm long as shown in **Fig. 2(a)**, and the second sheet was 1.52 m long as shown in **Fig. 2(b)**; in both cases the fibers were aligned with the direction of the beam axis and were designed to carry the equivalent tension in the internal reinforcing bars as if they had been fully developed. The design of the FRP composite rehabilitation for improving the joint shear capacity was determined by a procedure similar to that developed for T-joints in bridges

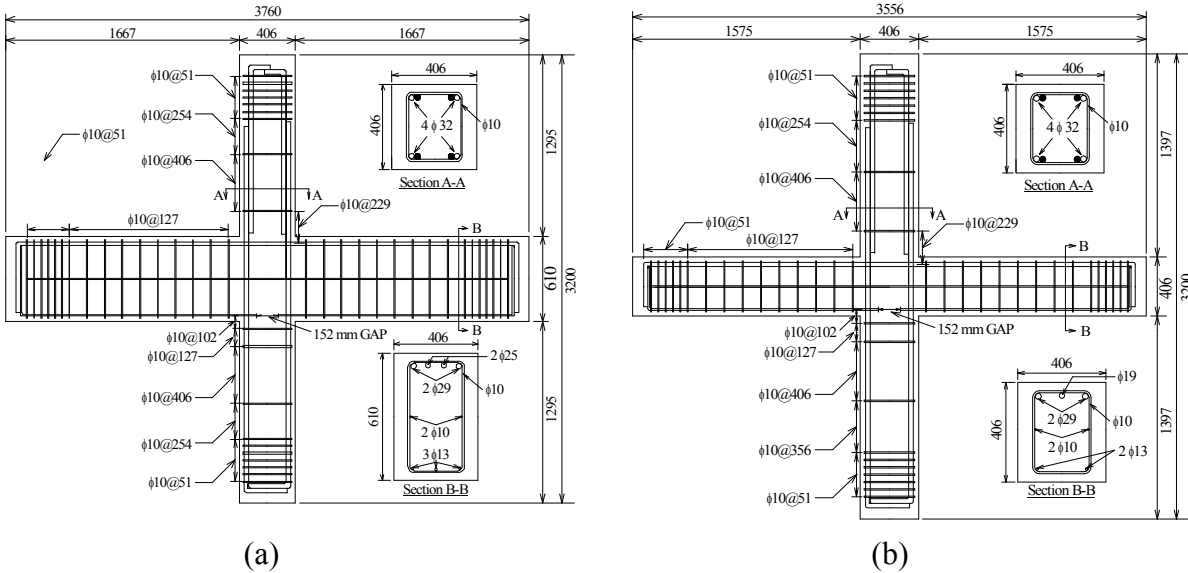


**Figure 1.** Joint specimen dimensions and reinforcement details: (a) Type I, (b) Type II.

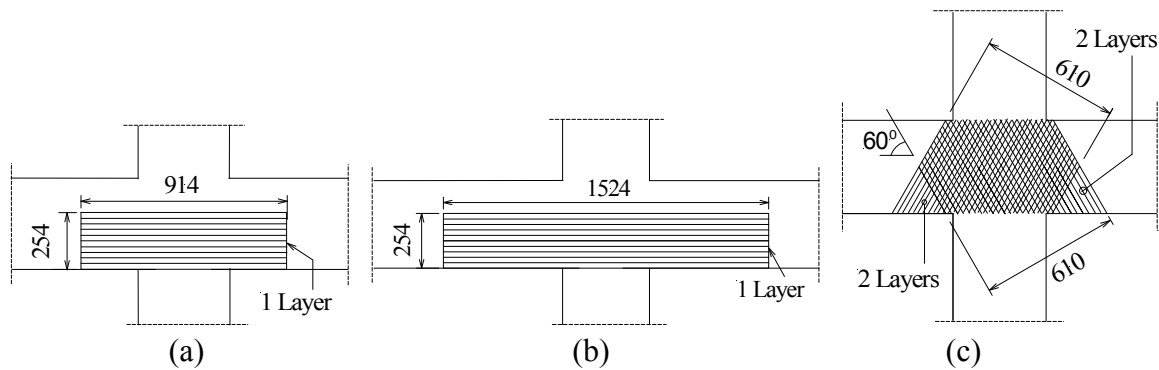


**Figure 2.** Elements of FRP rehabilitation: (a) short bond, (b) long bond, (c) joint shear.

(Pantelides et al. 1999, Gergely et al. 2000). The principal stresses and principal angle were determined in the joint and the width and thickness of the FRP composite fabric was then designed to increase the capacity of the joint in the direction of principal tension from a value known to cause cracking. Two FRP layers were placed at an angle of  $\pm 60^\circ$  from the horizontal in the joint region, as shown in **Fig. 2(c)**, on both faces of the joint to resist diagonal tensile stresses.

The flexural capacity of the top of the beams was 5.9 times that of the bottom of the beams for Type I joints; for Type II joints this ratio was 6.0 times. One carbon FRP composite sheet 406 mm wide and 914 mm long was placed on the bottom surface of each of the two beams framing into the joint, as shown in **Fig. 3(a)**. To minimize the potential for shear failure from occurring in the beams of the rehabilitated joint, two sheets of carbon FRP U-stirrups were used in the critical regions of the beams shown in **Fig. 3(b)**. The required number of sheets was found using established principles (ACI 440 200x) by ignoring the contribution of the concrete in the plastic hinge regions. No mechanical anchoring of the FRP U-stirrups was used. The FRP U-stirrups also served as anchorage of the CFRP lap splice sheets which were applied as shown in **Figs. 2(a, b)**. A general principle in seismic rehabilitation is that intervention for strengthening

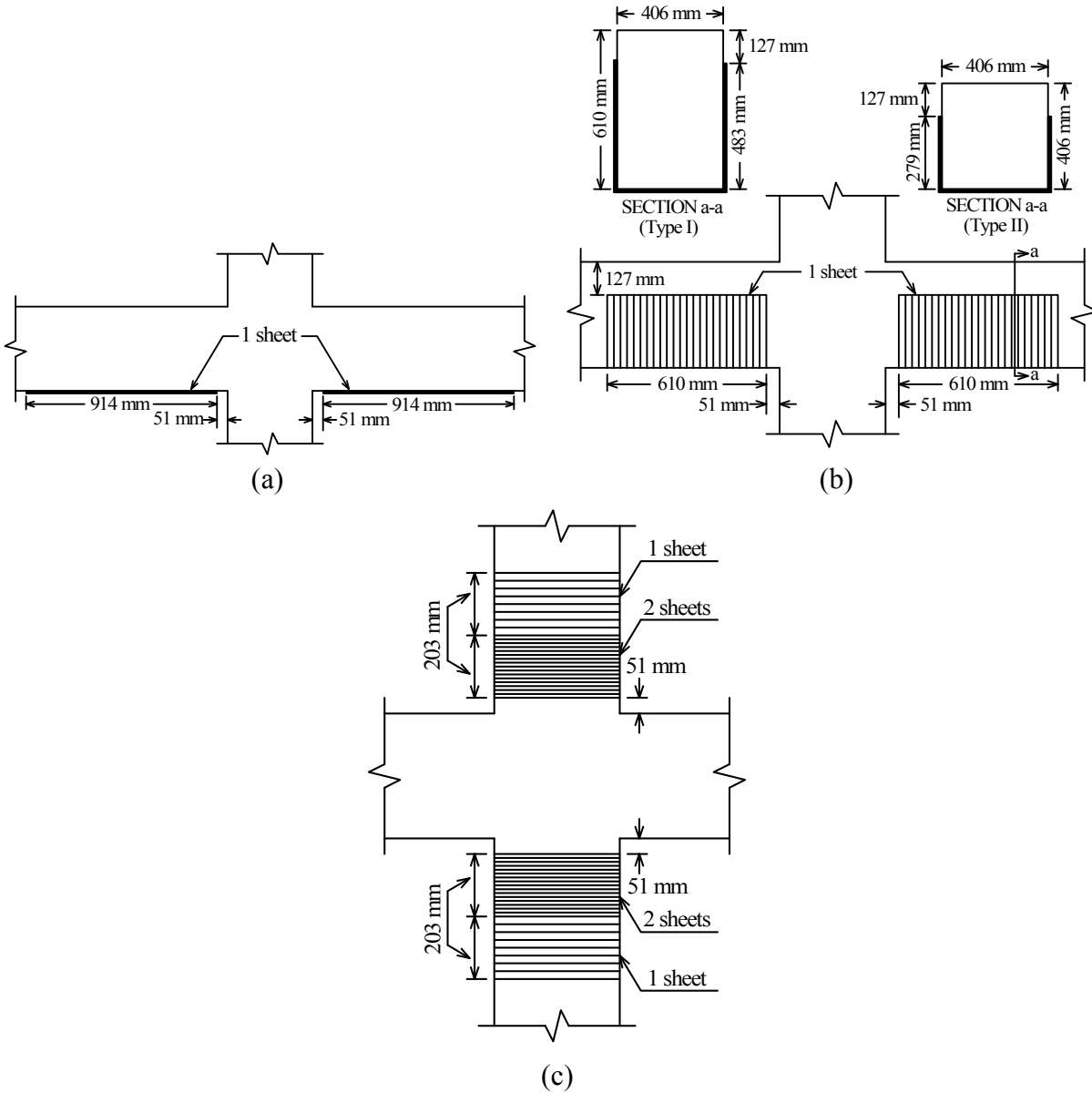


**Figure 3.** Additional elements of FRP rehabilitation: (a) beam flexural strengthening, (b) beam shear strengthening, (c) column confinement.

one portion of the structure should not force an undesirable brittle failure of another portion of the structure. To satisfy the strong-column weak-beam design criterion, the columns required strengthening for shear enhancement and confinement. Following design principles for column shear strengthening and confinement (Seible et al. 1997) two FRP sheets were found to be sufficient as shown in **Fig. 3(c)**; two sheets were applied in the hoop direction for the first 203 mm and one sheet for the subsequent 203 mm to distribute the stresses. The carbon FRP composite was terminated 51 mm from the beam face to allow independent rotation between the column and beams. The corners of the beams and the column were beveled to a 25 mm radius.

## Performance of As-built and Rehabilitated Interior Beam-Column Joints

The FRP rehabilitated joints achieved a higher drift ratio before ductile failure occurred compared to the as-built specimen that failed suddenly. The energy dissipation curves for Type I and Type II specimens are shown in **Fig. 4**. The cumulative energy dissipation for Type I FRP rehabilitated specimens was 2.3 times on average that of the as-built specimens. The cumulative energy dissipation for Type II FRP rehabilitated specimens was 1.2 times that of the as-built specimen. The failure modes for the rehabilitated specimens involved a bulging failure mechanism, whereby bulging of the concrete had spread over the entire joint region, as shown in **Fig. 5** for joints R24-3 and R16-2. The FRP composite jacket created a basketing effect of the fractured concrete inside the joint which allowed the specimen to carry compression forces well after cracking had developed in the joint concrete.

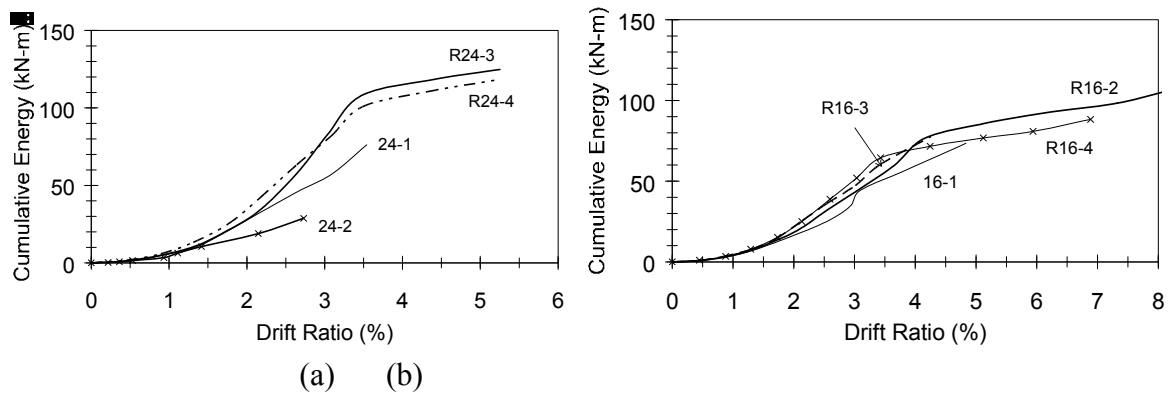


**Figure 4.** Cumulative energy: (a) Type I specimens : as-built (24-1, 24-2), rehabilitated (R24-3, R24-4); (b) Type II specimens: as-built (16-1), rehabilitated (R16-2, R16-3, R16-4).

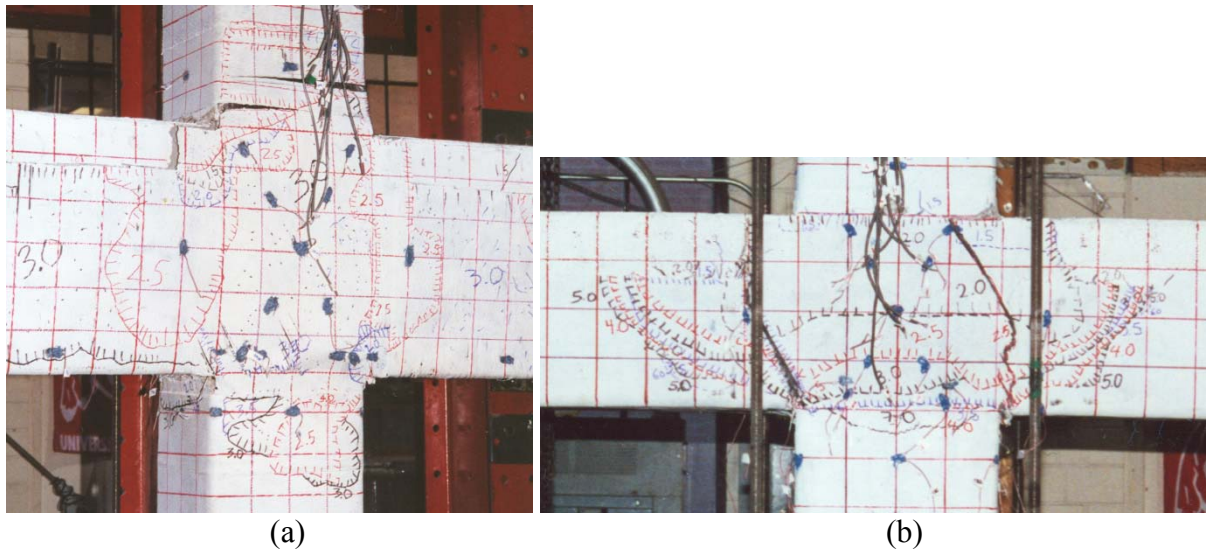


**Figure 5.** Failure modes of rehabilitated specimens: (a) Joint R24-3 (Type I), (b) Joint R16-2 (Type II).

A comparison of the analytical prediction of the bending moment capacity of the two beams framing into the joint with the experimental capacity was carried out. The analytical capacity was evaluated using actual material properties measured on the day of each test, such as the compressive strength  $f_{co}$ . From **Table 1**, it is clear that the two beams of the as-built specimens did not achieve the analytical bending moment capacity. However, the two beams of the rehabilitated Type I joints exceeded the analytical bending moment capacity by 12%-16%, and the two beams of the rehabilitated Type II joints exceeded the analytical bending moment capacity by 22%-54%.

**Table 1.** Analytical and experimental capacity of two beams in interior beam-column joints

Specimen	$f_{co}$ (MPa)	Beam Moments- Analysis (kN-m)	Beam Moments- Test (kN-m)	Test/ Analysis
Type I				
24-1	37.3	623.6	464.5	0.74
24-2	45.0	631.1	303.8	0.48
R24-3	48.0	633.4	733.6	1.16
R24-4	44.2	630.4	705.8	1.12
Type II				
16-1	39.0	267.6	250.4	0.94
R16-2	43.1	269.5	329.2	1.22
R16-3	49.0	271.6	350.5	1.29
R16-4	43.0	269.5	413.8	1.54

The joint shear strength coefficient,  $\gamma$ , is typically used to establish the joint shear capacity (ASCE 41 2006). It is defined in terms of the nominal joint shear strength as follows:

$$\gamma = \frac{V_n}{A_j f_{co}} \quad (1)$$

where  $V_n$  is the nominal joint shear strength and  $A_j$  is the effective horizontal joint area. **Fig. 6** shows that for Type I joints, the as-built specimens lost their joint shear capacity at a story drift ratio of 1.4%-2.6%; the rehabilitated Type I joint specimens did not lose joint shear capacity until a story drift ratio exceeding 4.3%. It is clear from **Fig. 7** that both the as-built and rehabilitated Type II specimens lost the joint shear capacity at a relatively low story drift ratio of 2.2%-2.9%; this is due to the bond-slip failure mode of the bottom beam bars.

**Table 2** compares the joint shear strength coefficient from ASCE 41 to the values obtained in the tests. From **Table 2** it is clear that the Type I as-built joints reach the ASCE 41 predicted joint shear strength. The Type I rehabilitated joints exceed the ASCE 41 predicted joint shear strength by 12%-21%. However, both the as-built and rehabilitated Type II joints do not reach the ASCE 41 predicted joint shear strength; this is obviously due to the premature bond-slip failure mode.

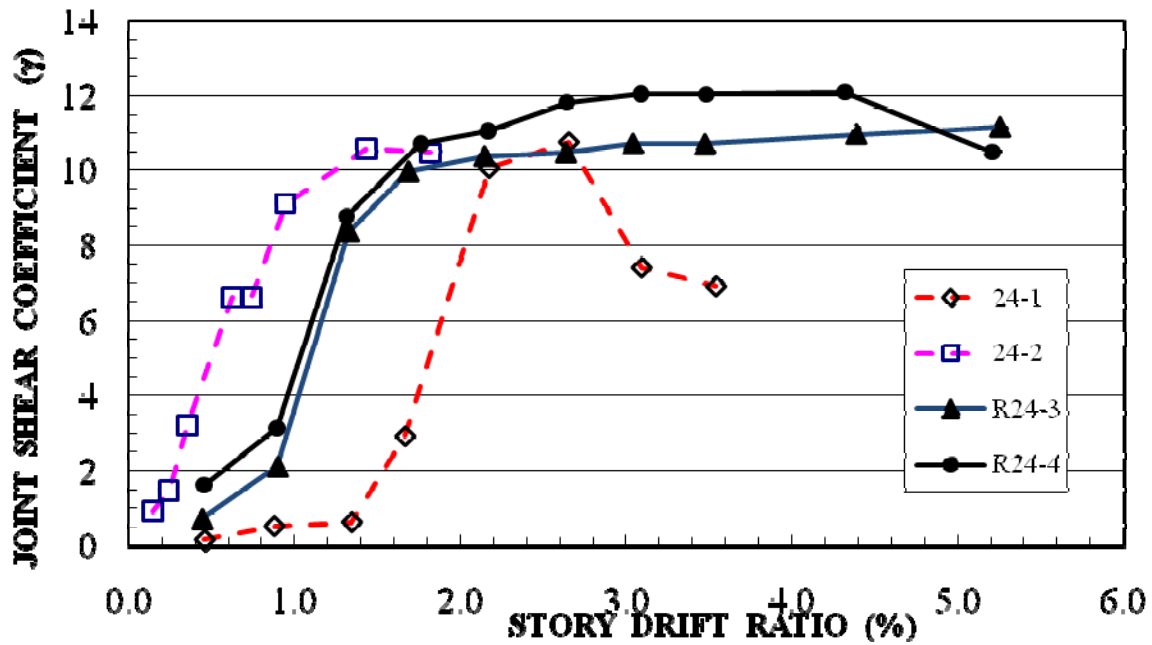


Figure 6. Joint shear strength coefficient for Type I interior beam-column joints.

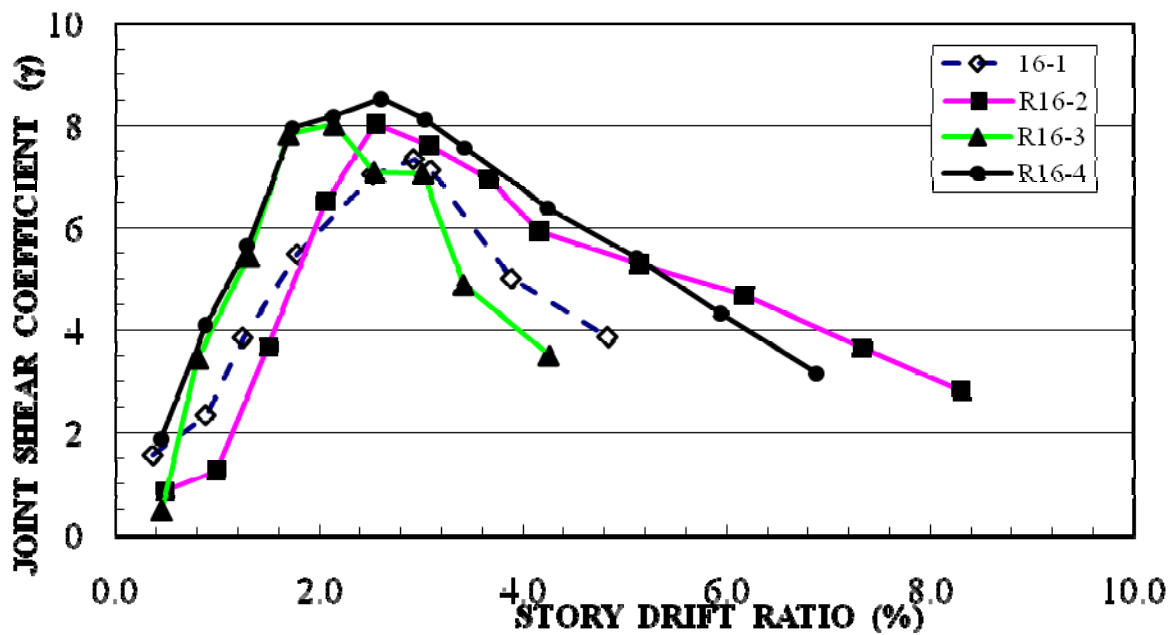


Figure 7. Joint shear strength coefficient for Type II interior beam-column joints.

**Table 2.** Joint shear strength coefficient of as-built and rehabilitated interior beam-column joints

Specimen	$\gamma$ (ASCE 41)		$\gamma$ (Tests)		$\gamma$ Tests/ ASCE 41
	(SI units)	(Customary units)	(SI units)	(Customary units)	
Type I					
24-1	0.833	10	0.896	10.75	1.075
24-2	0.833	10	0.881	10.57	1.057
R24-3	0.833	10	0.930	11.16	1.116
R24-4	0.833	10	1.008	12.10	1.210
Type II					
16-1	0.833	10	0.613	7.35	0.735
R16-2	0.833	10	0.671	8.05	0.805
R16-3	0.833	10	0.683	8.20	0.820
R16-4	0.833	10	0.712	8.54	0.854

### Strut-and-Tie Models for the As-built and FRP-rehabilitated Joints

An equilibrium-based strut-and-tie model was developed in this research which was supplemented with strain readings from the internal steel reinforcement and external FRP composite laminates. For a Strut-and-Tie (STM) model to be valid, equilibrium has to be satisfied at each node. Since the seismic force is cyclic in nature, the STM model for the present case must be developed for both positive and negative forces and displacements. Since the displacements are identical because of symmetry, a positive case was chosen and a STM model was developed as shown in **Fig. 8(a)**.  $P_1$ ,  $P_2$ ,  $P_3$  and  $P_4$  are external forces that can be obtained by experimental data or structural analysis.  $P_C$  is a compressive force that acts on the strut, and  $\theta_C$  is the angle between the horizontal plane and the centerline of the strut. The STM model for the rehabilitated joints is shown in **Fig. 8(b)**.  $P_D$  and  $P_\phi$  are the tensile forces that act on the diagonal and horizontal ties respectively.  $\theta_D$  is the angle between the horizontal plane and the centerline of the tie. Geometric and strut width constraints were implemented for the STM model of **Fig. 8**. The equilibrium equations must be satisfied and the concrete strut capacity must not be exceeded for the model to work. In addition, the width of the horizontal and diagonal sheets must not exceed the actual dimensions of the FRP composite that was applied in the tests. A reanalysis of the assumed model is iterated by checking the tolerance of angle  $\theta_C$ ; all requirements are satisfied to the degree of the percentage error. The results of the analysis of the STM model of the as-built specimens and FRP rehabilitated specimens shows that the STM models work within an error of less than 10%.

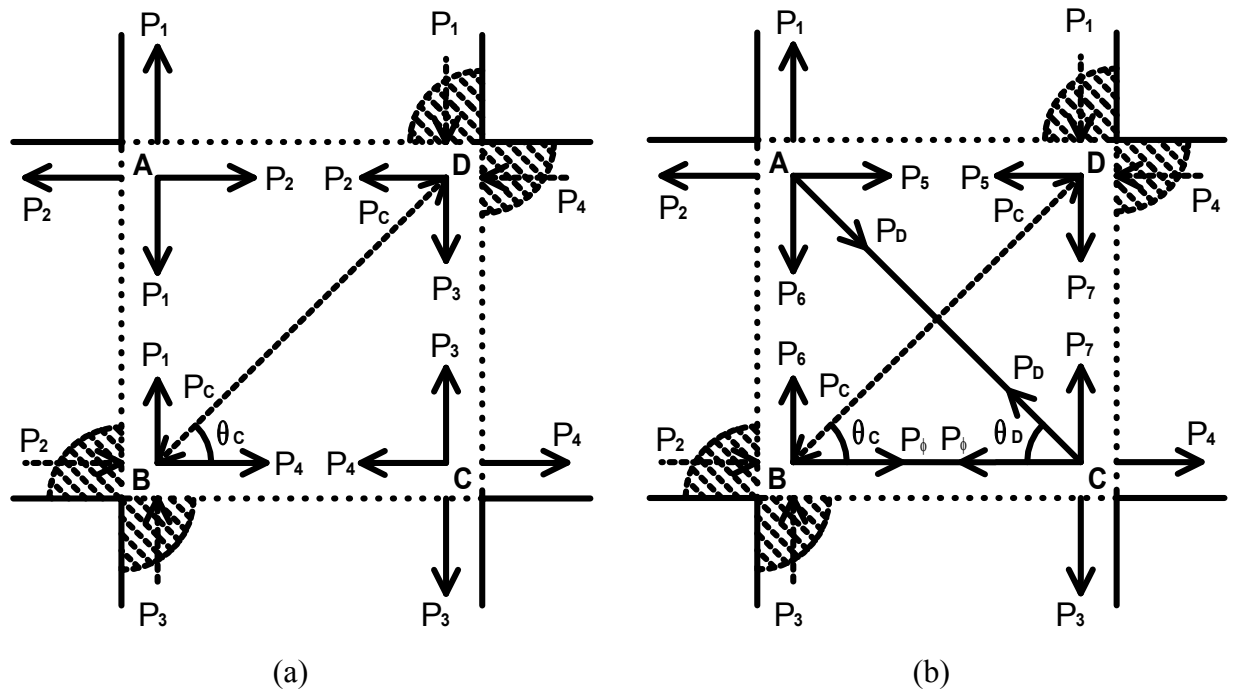


**Figure 8.** Strut-and-tie models: (a) as-built specimens, (b) FRP rehabilitated specimens.

### Conclusions

The rehabilitation measures were successful in promoting ductile behavior by delaying brittle joint shear failure and pullout of the beam bottom steel bars at the joint. The basketing effect of the FRP composite jacket allowed the fractured concrete in the joint to carry compression forces well after cracking had developed in the concrete. These measures delayed the propagation of damage in the joint panel and postponed the loss of stiffness and strength. The cumulative energy dissipation for Type I rehabilitated joints reached 2.3 times the average of the as-built joints, while for Type II rehabilitated joints it only reached 1.2 times the average of the as-built specimens. For both Type I and Type II joints, the two beams of the as-built specimens did not achieve the analytical bending moment capacity. However, the two beams of the rehabilitated Type I joints exceeded the analytical bending moment capacity by 12%-16%, and the two beams of the rehabilitated Type II joints exceeded the analytical bending moment capacity by 22%-54%. The Type I rehabilitated joints exceeded the ASCE 41 predicted joint shear strength by 12%-21%; in addition the rehabilitated Type I joint specimens did not lose joint shear capacity until a story drift ratio exceeding 4.3%. However, both the as-built and rehabilitated Type II joints did not reach the ASCE 41 predicted joint shear strength, which is attributed to premature bond-slip failure of the bottom beam bars.

An equilibrium-based strut-and-tie model was developed for the as-built and FRP rehabilitated joints, which was supplemented with strain readings from the internal steel reinforcement and external FRP composite laminates. The results of the analysis of the STM model of the as-built joints and rehabilitated joints shows that the STM models work within an error of less than 10%.

## References

- ACI Committee 440. (2008). "440.2R-08. Guide for the Design and Construction of Externally Bonded FRP Systems for Strengthening Concrete Structures" Farmington Hills, MI.
- American Society of Civil Engineers (2006). "ASCE/SEI 41-06. Seismic Rehabilitation of Existing Buildings." Reston, VA.
- Al-Salloum, Y.A., and Almusallam, T.H. (2007). "Seismic response of interior beam-column joints upgraded with FRP sheets. I: Experimental study." *J. Compos. Constr.*, 11(6), 575-589.
- Antonopoulos, C.P., and Triantafillou, T.C. (2003). "Experimental investigation of FRP-strengthened RC beam-column joints." *J. Compos. Constr.*, 7(1), 39-49.
- Clyde, C., and Pantelides, C.P. (2002). "Seismic evaluation and rehabilitation of R/C exterior building joints." *Proc. 7<sup>th</sup> U.S. National Conf. Earthq. Engrg.*, Boston, (CD-ROM).
- Gergely, I., Pantelides, C.P., and Reaveley, L.D. (2000). "Shear strengthening of R/C T-joints using CFRP composites", *J. Compos. Constr.*, 4(2), 56-64.
- Ghobarah, A., and El-Amoury, T. (2005). "Seismic rehabilitation of deficient exterior concrete frame joints." *J. Compos. Constr.*, 9(5), 408-416.
- Ghobarah, A., and Said, A. (2002). "Shear strengthening of beam-column joints." *Engineering Structures*, 24(7), 881-888.
- Mosallam, A.S., (2000). "Strength and ductility of reinforced concrete moment frame connections strengthened with quasi-isotropic laminates." *Composites Part B: Engineering*, 31(6-7), 481-497.
- Pampanin, S., Bolognini, D., and Pavese, A. (2007). "Performance-based seismic retrofit strategy for existing reinforced concrete frame systems using fiber-reinforced polymer composites." *J. Compos. Constr.*, 11(2), 211-226.
- Pantelides, C.P., Gergely, I., Reaveley, L.D., and Volnyy, V.A. (1999). "Retrofit of R/C bridge pier with CFRP advanced composites", *J. Struct. Engrg.*, 125 (10), 1094-1099.
- Prota, A., Nanni, A., Manfredi, G., and Cosenza, E. (2004). "Selective upgrade of under-designed reinforced beam-column joints using carbon fiber-reinforced concrete." *ACI Structural J.*, 101(5), 699-707.
- Seible, F., Priestley, M.J.N., Hegemier, G.A., Innamorato, D., (1997). "Seismic retrofit of RC columns with continuous carbon fiber jackets", *J. of Comp. Constr.*, 1(2), 52-62.